Structure, Volume *27*

Supplemental Information

Structure, Function, and Dynamics of the Gα Binding Domain of Ric-8A

Baisen Zeng, Tung-Chung Mou, Tzanko I. Doukov, Andrea Steiner, Wenxi Yu, Makaia Papasergi-Scott, Gregory G. Tall, Franz Hagn, and Stephen R. Sprang

Table S1.
Solvent accessible surface of, and spatial relationships between ARM and HEAT repeats of R432; Related to Figure 2B

Intra-repeat parameters				Inter-repeat parameters			
repeat	residue range	Repeat type	Intra-repeat SASA* ($Å^2$)	transition	Rotation (°)	Center-Center (Å)	Inter-repeat SASA ($Å^2$)
1	1-36	H	836	-	-	-	
2	37-76	H	953	1→2	39	10.6	2043
3	77-128	A	1415	2→3	22	9.8	1978
4	129-174	A	1338	3→4	31	10.9	2191
5	175-236	A	1695	4→5	34	11.3	2342
6	237-282	H	1200	5→6	40	11.4	2490
7	283-344	A	2250	6→7	78	13.3	1948
8	345-400	A	1791	7→8	61	12.7	2193
9	401-429	H	556	8→9	114	11.7	1551

* Solvent Accessible Surface Area, computed using Mac PyMol version 1.7 Schödinger LLC. Rotation and translations were determined using the PyMol script *draw_rotation_axis* available at https://raw.githubusercontent.com/Pymol-Scripts/Pymol-script-repo/master/draw_rotation_axis.py

Table S2.

Fit of Models from SREFLEX normal-mode fitting of pR452 crystal structure to SAXS curves for phosphorylated (P01-5) and non-phosphorylated R452 (U01-5); Related to Figure 4

model	Rotation of Segment 1 (°)*	Rotation of Segment 3 (°)*	RMSD (Å)	χ^2	clash	breaks
P-01	13.64	25.02	3.66	.24	.09	.03
P-02	16.68	20.43	4.03	.26	0	0
P-03	12.5	12.0	3.08	.27	0	.01
P-04	28.9	48.99	9.71	.27	.14	.18
P-05	12.3	15.19	3.66	.28	0	0
U-01	9.56	26.31	6.05	.39	0	.27
U-02	24.57	26.21	5.78	.44	05	.19
U-03	21.56	34.14	7.71	.44	05	.42
U-04	16.74	21.27	3.95	.44	0	0
U-05	3.59	23.25	5.08	.44	.14	,18

* Magnitude of rotation of Segment 1 (residues 1-183) or Segment 3 (residues 288-430) relative to Segment 2 (residues184-287) of the native crystal structure; RMSD between Cα positions of the molecule B of pR452 and corresponding atoms of the model. Clash and break scores indicate the relative number of steric overlaps within the model structure and breaks in the polypeptide chain, respectively (Panjkovich and Svergun, 2016).

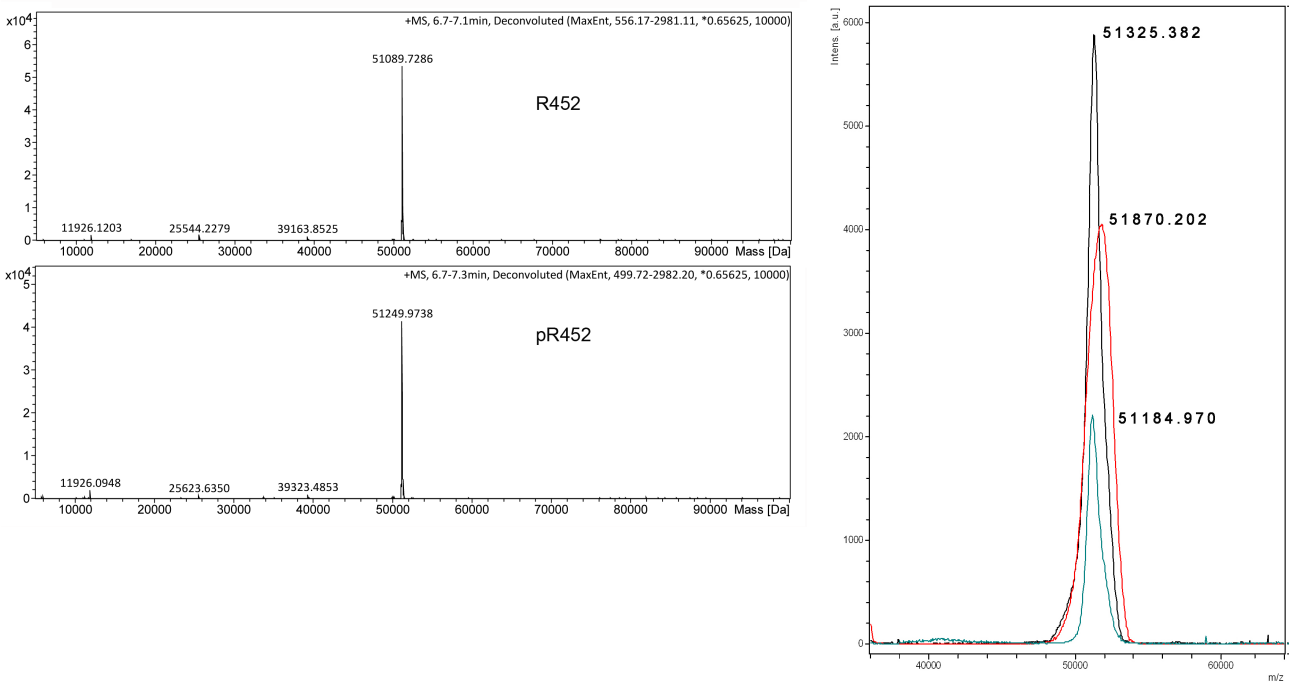

Figure S1. Casein Kinase II phosphorylates R452 at two sites. Related to Figure 1 and Figure 2. See STAR Methods for phosphorylation and Mass Spectrometry protocols. (A) triple quadrupole mass spectrometric analysis of phosphorylated and unphosphorylated Ric-8A The mass difference between R452 and pR452 is 160.249 Da, consistent with phosphorylation at two sites. (B) MALDI-TOF mass spectrometry of dissolved crystals of pR452 crystals (red), purified R452 (cyan) and pR452 (black). Mass spectrometry experiments were performed using a microflex MALDI-TOF (Bruker) with flexControl (Bruker) software. Data was analyzed using flexAnalysis (Bruker) software.

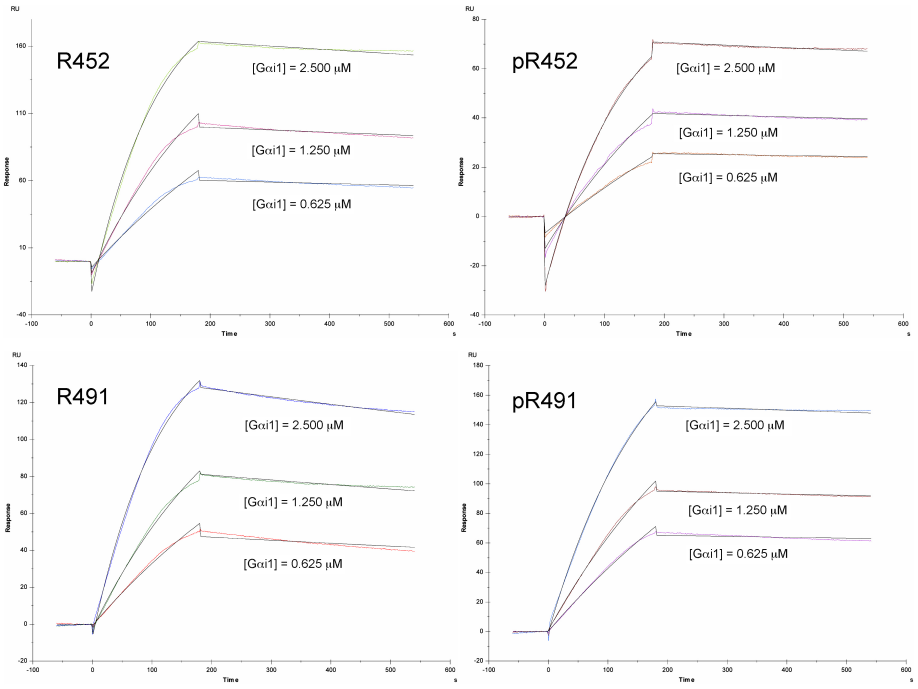

Figure S2. Kinetics of Ric-8A protein binding to Gαi1 measured by surface plasmon resonance using a BiaCore X100 system (GE Healthcare). See STAR Methods. Related to Figure 1. N-terminally hexa-histidine-tagged Ric-8A ligands (R452, pR452, R491, pR491) were anchored to an Ni-NTA sensor chip surface for 5 minutes For The Gαi1•GDP analyte was applied to the ligand-coated sensor chip surface at each of a range of concentrations (0.625 μM, 1.25μM, 2.5μM). Binding and dissociation data were globally fit to a 1:1 binding model to generate a single k_{on} and k_{off} (See STAR Methods). Note that k_{on} is an apparent pseudo-first order association rate ($M^{-1}s^{-1}$), and k_{off} is the dissociation rate (s^{-1}). The apparent on-rate includes the kinetics of GDP dissociation from Gαi1, such that Gαi1•GDP is the species that associates with the chip-bound Ric-8A ligands, whereas it is nucleotide-free Gαi1 that dissociates from ligand. Thus, the ratio k_{off}/k_{on} is not equivalent to the dissociation constant for the Ric-8A:Gαi1•GDP complex.

Ligand	$k_{on,\ apparent}$ ($M^{-1}s^{-1}$)	k_{off}, (s^{-1})
R452	3302 (205)	1.52 (0.04) x 10^{-4}
pR452	2664 (277)	1.13 (0.04) x 10^{-4}
R491	3190 (243)	3.04 (0.04) x 10^{-4}
pR491	2614 (424)	8.94 (0.3) x 10^{-5}

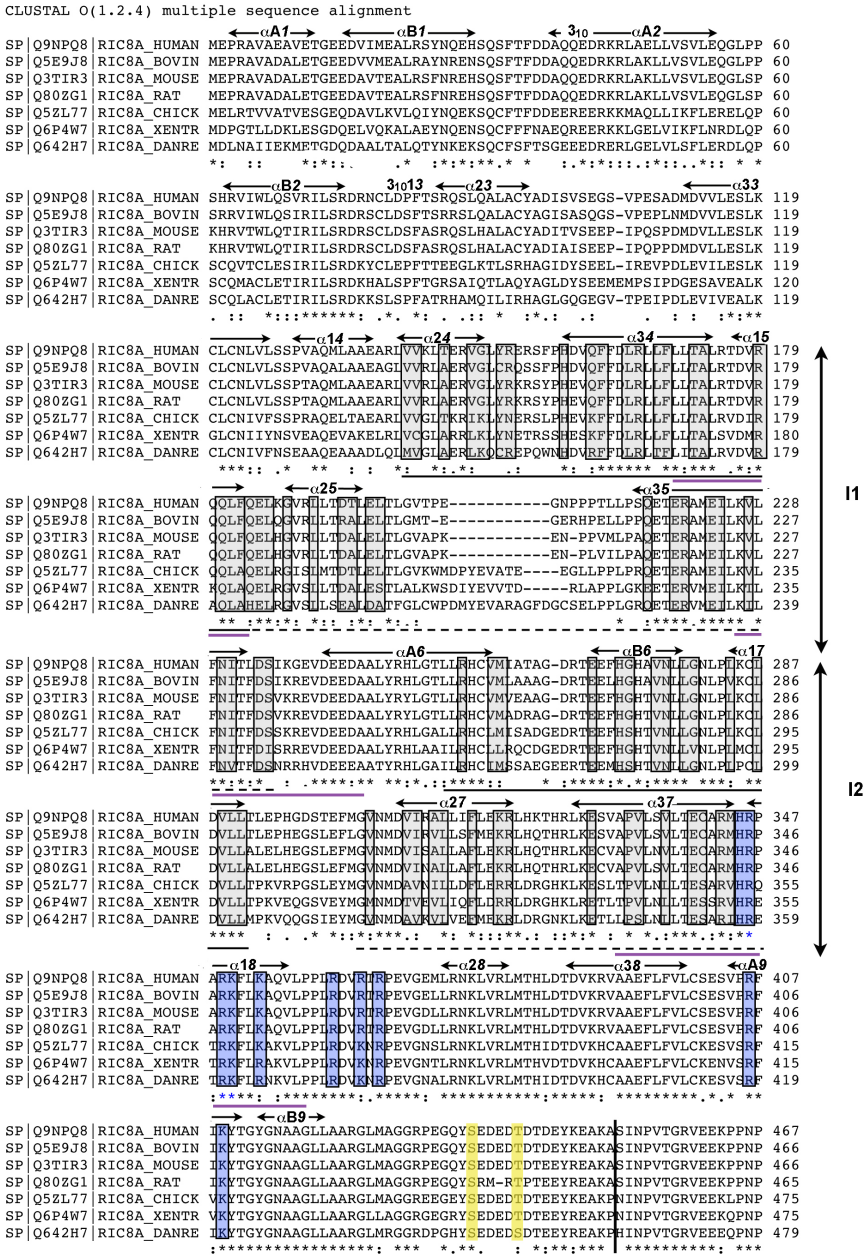

Figure S3. Amino acid sequence alignment of Ric-8A homologs (human, bovine, mouse, rat, chicken, frog (xenopus), zebrafish). Related to Figures 2, 4, and 5. Amino acids at interface between subdomain interfaces are boxed in gray, with black and dashed underlines lines indicating residues at opposing interfaces, I1 between subdomains (1-183) and (184-287) and I2, between subdomains (184-287) and (288-429), demarcated with vertical lines at right. Magenta underlining indicates segments of strongest protection from HDX (Figures 2, 5). Residues in the conserved basic region (Figure 2C, 5C) are shown in blue-shaded boxes. Extent of secondary structure elements of HEAT/ARM repeats are shown above sequence blocks. Phosphorylated residues Ser335 and Thr440 are shaded in yellow. Alignment performed using European Bioinformatics Institute CLUSTALW server https://www.ebi.ac.uk/Tools/msa/clustalo/ from sequences deposited in the UniProtKb database https://www.uniprot.org/.

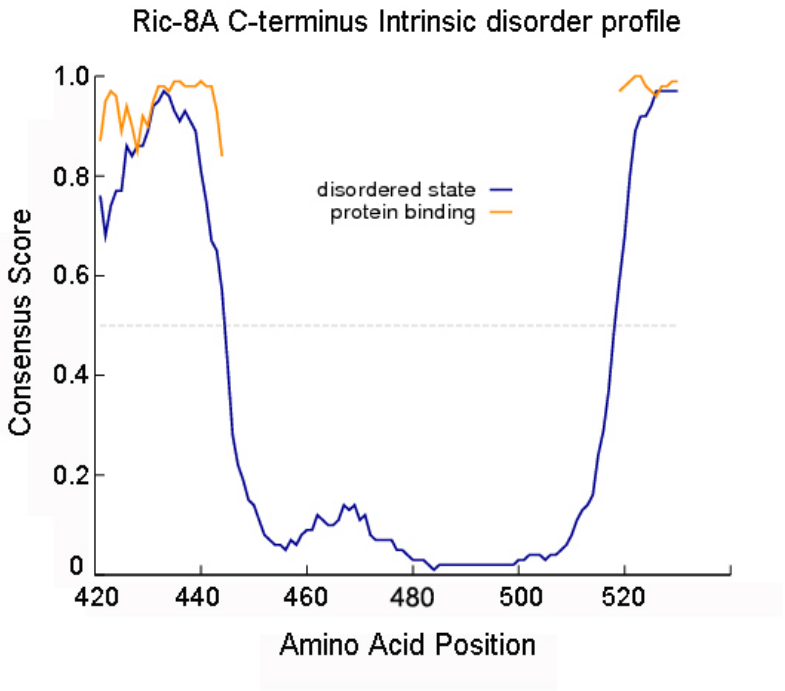

Figure S4. Prediction of disordered residues by DISOPRED-3 (Jones and Cozzetto, 2015). Related to Figure 2 and Figure 4. The grey dashed line indicates a confidence score of 0.5, above which the input sequence is considered disordered. The orange line shows the confidence of disordered protein binding residue predictions. DISOPRED-3 was accessed through the PSIPRED server http://bioinf.cs.ucl.ac.uk/psipred/?disopred=1

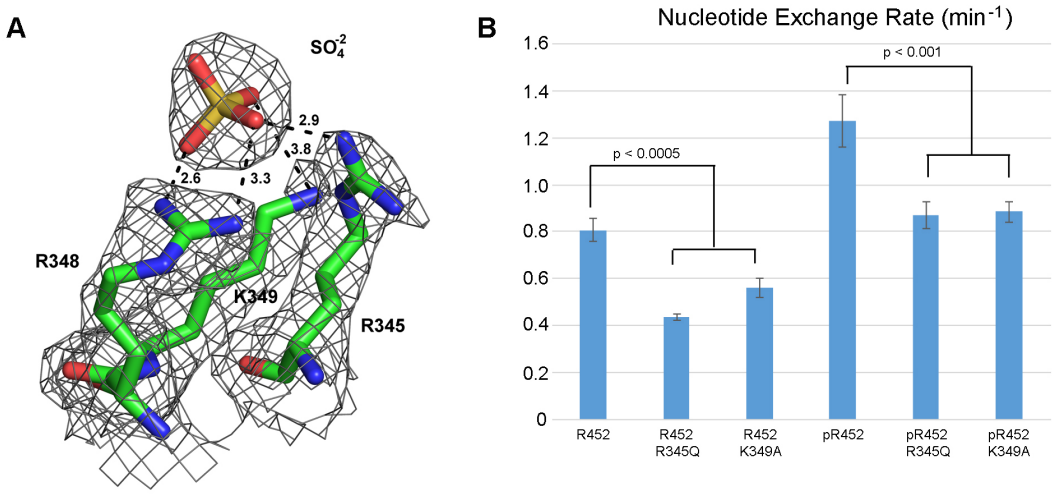

Figure S5. A potential phosphate-binding site near the N-terminus of $\alpha 1$*8* composed or R345 and R348 of pR452, bound to a sulfate ion derived from crystallization buffer. Related to Figure 2 (A) The 2mFo-DFc map calculated with the final, refined phase set, is rendered at the 1.0 σ contour level. Carbon atoms are colored *green*, nitrogen, *blue*, oxygen, *red*, sulfur, *yellow*. Interatomic contact distances shown with dashed lines with distances in Ångstrom units, Rendered using PyMOL V1.7, Schrödinger, LLC. Average B factors for guanidinium groups of Arg345 and Arg348 are 57Å^2 and 46Å^2, respectively. The B factor for the Nζ of Lys349 is 56Å^2. The overall B factor for the sulfate ion is 75Å^2. These may be compared to the average B factor for all protein atoms, 47Å^2. (B) Fluorimetric Guanine nucleotide exchange assay, conducted as described in (Kant, et al, 2016). See STAR Methods. Exchange reactions were conducted in buffer (50mM HEPES pH 8.0, 1 mM TCEP, 150 mM NaCL and 10 mM$MgCl_2$) containing 10 mM GTPγS, 2μM R452 or pR452 or mutants thereof as indicated, and 2μM Gαi1 at a reaction temperature of 25° Reaction volume was 500μl. Reaction was initiated by addition of Gαi1•GDP to R452 mixture and Gαi1•GTPγS measured by fluorescence emission at 345nm (excitation wavelength 295nm) in an LS55 luminescence spectrometer (PerkinElmer Life Sciences). Three to 5 replicates were taken for each data set and significance of differences was estimated by a Student's T-Test.

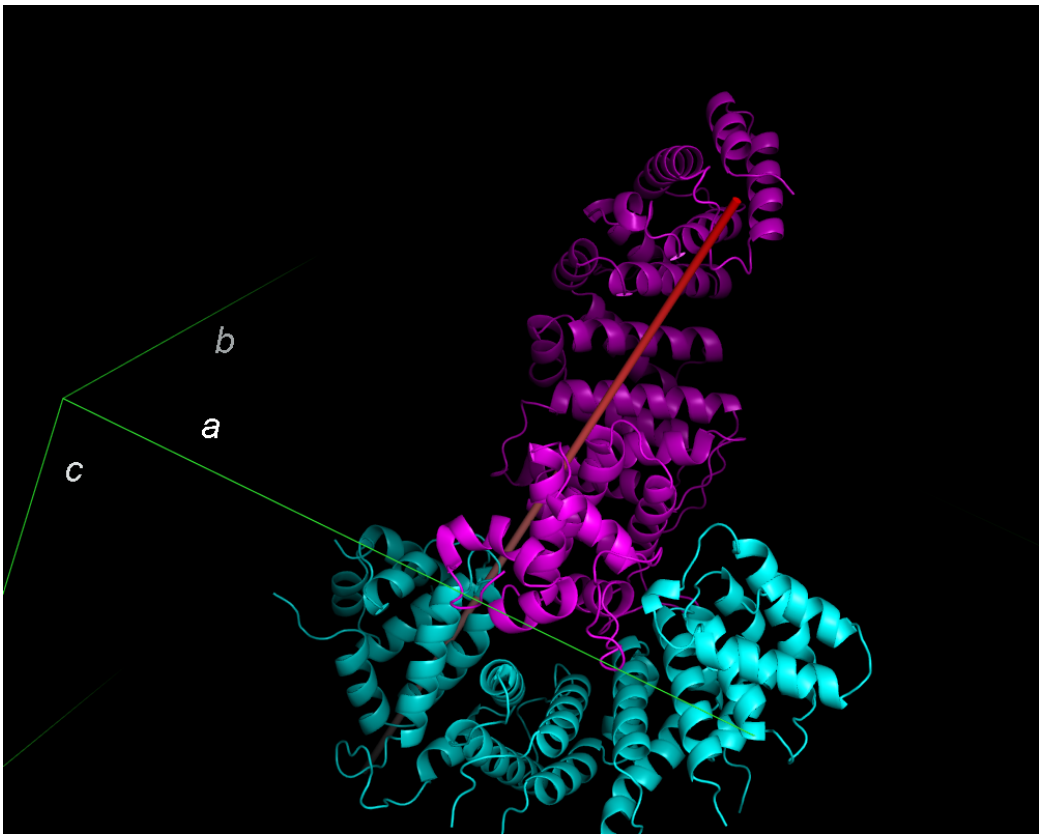

Figure S6 Symmetry relationship and packing interactions between pR452 molecules A and B. Related to Table 1 and Figure 2. The red line shows the screw axis that relates the two molecules in the asymmetric unit by a 110° rotation and a translation of 29Å. This packing interaction arises from an extensive interface formed by α1*8* and αA*9* motifs of molecule B with the C-shaped cavity formed by multiple ARM/HEAT repeats of molecule A. The corresponding surface of molecule B forms similar, but less intimate contacts with the α1*8* and αA*9* motifs of a symmetry-related copy of Molecule A. The rms deviation between the Cα atoms of molecule A and molecule B is 0.78 Å (346 atoms aligned). The PyMOL script *draw_rotation_axis* available at https://raw.githubusercontent.com/Pymol-Scripts/Pymol-script-repo/master/draw_rotation_axis.py was used to compute the superposition matrix and derive screw-axis parameters.

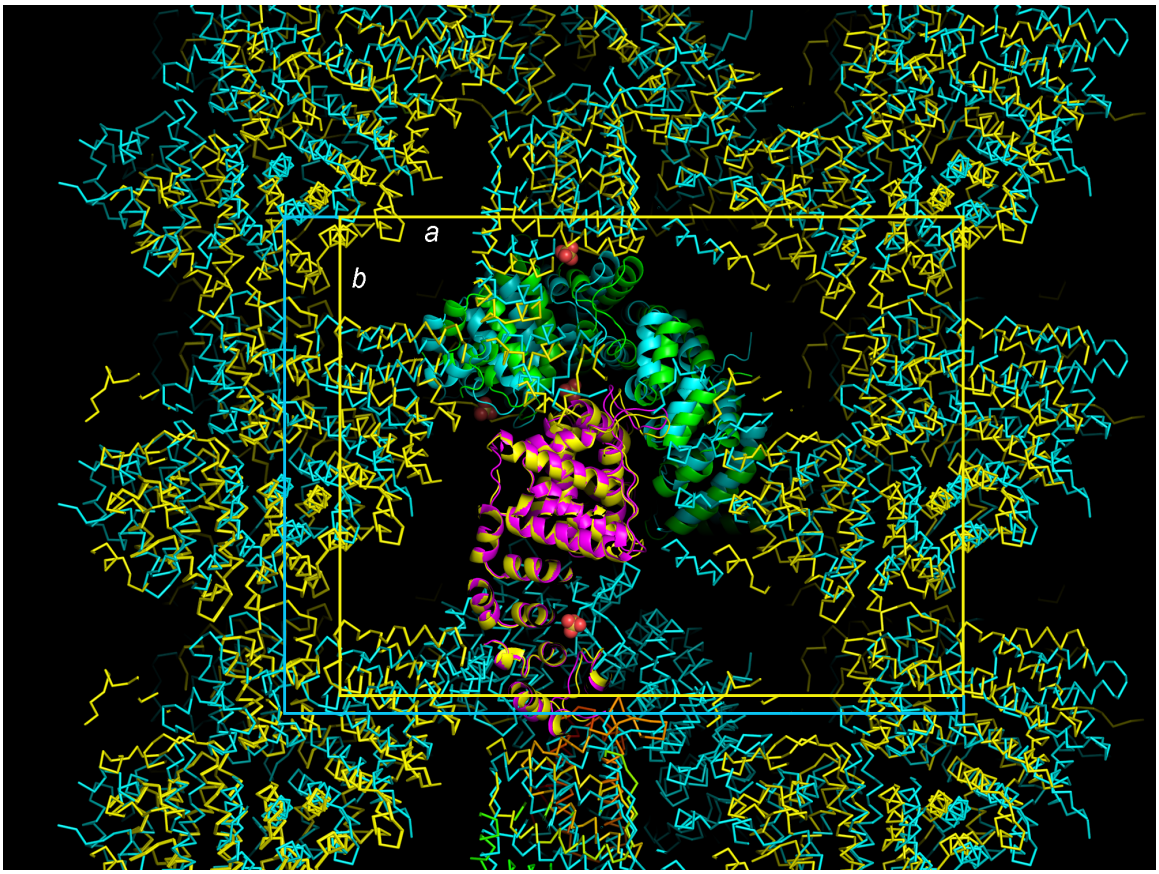

Figure S7. Immersion of pR452 crystals in paratone-N (Hampton) causes lattice contraction along all three unit cell axes. Related to Table 1. The crystal lattices of the native and paratone-N-soaked crystals and their contents are colored *cyan* and *yellow*, respectively and aligned by superposition of molecule B (symmetry equivalent *x,y,z*) of the native structure (cartoon ribbon colored *magenta*) with the corresponding molecule in the paratone-N-soaked crystals (cartoon ribbon colored *yellow*). Molecules A are shown as *cyan* (native crystals) and *green* (paratone) ribbons. Sulfate ions that are present in native, but not paratone-N soaked crystals are shown as van der Waals spheres. Oil immersion causes changes in packing interactions (including those between molecules A and B), but only minor distortion of pR452 itself (rms differences at Cα positions = 0.63Å (365 atoms aligned) and 0.64Å (344 atoms aligned) for chains A and B, respectively, relative to their counterparts in native crystals). Figure produced using Mac PyMOL, Version 1.7 Schrödinger LLC.

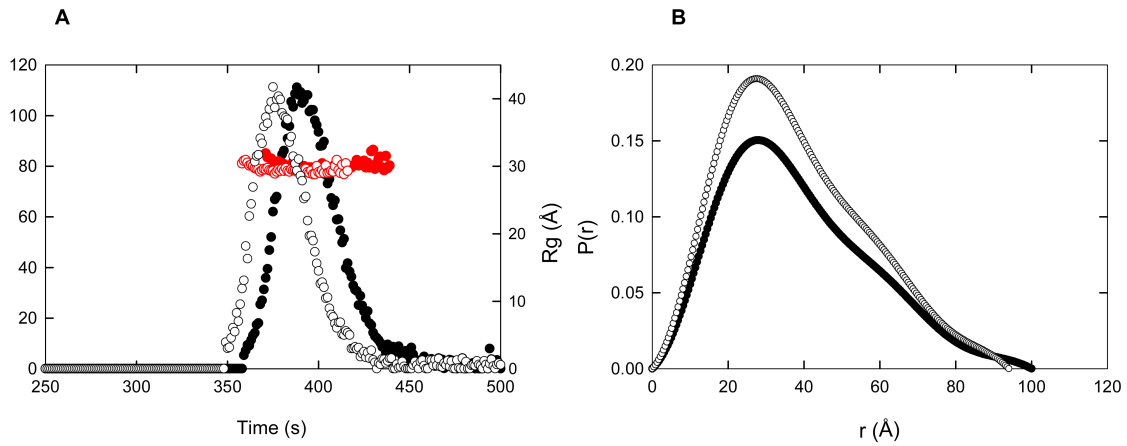

Figure S8. (*A*) SEC-SAXS chromatography of R452 (closed circles) and pR452 proteins (open circles); *I*(0) (black) and *R*g (red) are plotted as a function of time as sample passing through the S200 Increase 1.3/300 column. (*B*) pair distribution function, *P*(r), computed using the GEOM indirect transform program in the ATSAS program suite. Related to Table 2 and Figures 3 and 4.